References

1. E. M. Simon and B. H. Zimm, *J. Stat. Phys.* **1**, 41 (1969); E. M. Simon, *J. Chem. Phys.* **51**, 4937 (1969).
2. J. H. Weiner and R. E. Forman, *Phys. Rev. B* **10**, 315 (1974).
3. D. L. Ermak, *J. Chem. Phys.* **62**, 4189, 4197 (1975).
4. D. L. Ermak and H. Buckholtz, *J. Comput. Phys.* **35**, 169 (1980).
5. M. P. Allen, *Mol. Phys.* **47**, 599 (1982); *ibid.* **40**, 1073 (1980).
6. W. F. van Gunsteren and H. J. C. Berendsen, *Mol. Phys.* **45**, 637 (1982); *ibid.* **44**, 69 (1981).
7. S. Lee, Ph. D. Thesis, Harvard University, 1986.
8. D. L. Ermak and J. A. McCammon, *J. Chem. Phys.* **69**, 1352 (1978); the algorithm derived in this paper is limited to the diffusive regime (*i.e.*, $\Delta t \gg \gamma^{-1}$).
9. P. Turq, F. Lantelme, and H. L. Friedman, *J. Chem. Phys.* **66**, 3039 (1977).
10. G. Ciccotti and J.-P. Ryckaert, *Mol. Phys.* **40**, 141 (1980); G. Ciccotti, M. Ferrario, and J.-P. Ryckaert, *ibid.* **46**, 875 (1982).
11. F. J. Vesely, *Mol. Phys.* **53**, 505 (1984).
12. J. A. Montgomery, Jr., D. Chandler, and B. J. Berne, *J. Chem. Phys.* **70**, 4056 (1979).
13. H. Brenner, *J. Colloid, Sci.* **20**, 104 (1965); *ibid*, **23**, 407 (1967).
14. E. Dickinson, S. A. Allison, and J. A. McCammon, *J. Chem. Soc., Faraday Trans. II* **81**, 591 (1985).
15. D. W. Condiff and J. S. Dahler, *J. Chem. Phys.* **44**, 3988 (1966).
16. P. G. Wolynes and J. M. Deutch, *J. Chem. Phys.* **67**, 733 (1977); J. A. Montgomery, Jr. and B. J. Berne, *J. Chem. Phys.* **67**, 4589 (1977); J. A. Montgomery, Jr., B. J. Berne, P. G. Wolynes, and J. M. Deutch, *J. Chem. Phys.* **67**, 5971 (1977).
17. G. Ciccotti and J.-P. Ryckaert, *J. Stat. Phys.* **26**, 73 (1981); G. Bossis, B. Quentrec, and J. P. Boon, *Mol. Phys.* **45**, 191 (1982).
18. W. F. van Gunsteren and H. J. C. Berendsen, *Mol. Phys.* **47**, 721 (1982).
19. Use, for example, GGNML subroutine in the IMSL Library; IMSL Library 9 Reference Manual (IMSL International Mathematical and Statistical Libraries, Inc., Houston, Texas, 1982).
20. D. M. Brink and G. R. Satchler, Angular Momentum, 2nd ed. (Oxford University Press, London, 1968).
21. H. Goldstein, Classical Mechanics (Addison-Wesley, Reading, Massachusetts, 1959), p.141; the definition of the Euler angles (ϕ, θ, ψ) given in this reference are related to (α, β, γ) by $\phi = \alpha + \pi/2$, $\theta = \beta$, and $\psi = \gamma - \pi/2$.
22. A similar procedure has been used in molecular dynamics simulations of systems of nonspherical molecules; see, for example, J. Barojas, D. Levesque, and B. Quentrec, *Phys. Rev. A* **7**, 1092 (1973).
23. Eq. (4-102) of Ref. 21.
24. P. Mazur and W. van Saarloos, *Physica A* **115**, 21 (1982).
25. U. Steiger and R. F. Fox, *J. Math. Phys.* **23**, 296 (1982).
26. J. Garcia de la Torre and V. A. Bloomfield, *Quart. Rev. Biophys.* **14**, 81 (1981); J. M. Garcia Bernal and J. Garcia de la Torre, *Biopolymers* **19**, 751 (1980).
27. S. Lee and M. Karplus, *J. Chem. Phys.* **81**, 6106 (1984).

Different Mode of Cytochrome *c* and Apocytochrome *c* Interactions with Phospholipid Bilayer

Seungcheol Lee and Hyoungman Kim*

Department of Biological Science and Engineering, The Korea Advanced Institute of Science, Seoul 130-650. *Received November 10, 1989*

Cytochrome *c* induces fusion of phosphatidylserine/phosphatidylethanolamine vesicles while apocytochrome *c* does not have a fusogenic capability despite the fact that the apoprotein binds to the vesicles more extensively. In order to see whether the difference in the fusogenic behavior comes from the topological variation in membrane bound proteins, the holoprotein and apoprotein were labeled with phenylisothiocyanate, a hydrophobic label, in the presence of its hydrophilic analogue *p*-sulfophenylisothiocyanate. Apocytochrome *c* was labeled with the hydrophobic probe more extensively than the cytochrome *c*, indicating that the apoprotein penetrates deeper into the bilayer than cytochrome *c* does. The translocation experiments of these proteins by trypsin entrapped vesicles further supported this conclusion.

Introduction

The studies on fusion of phosphatidylserine/phosphatidylethanolamine (PS/PE, 1:1, mol/mol) vesicles induced by α-lactalbumin[1-3] and lysozyme[4] suggested that surface penetration of small protein segments is important for the process. Apocytochrome *c* (Apo *c*) binds more extensively to PS/PE vesicles and a longer stretch of it is protected from the proteolysis of the protein-vesicle complex as compared

*To whom correspondence should be addressed.

to cytochrome *c* (Cyt *c*). It was found, however, that Apo *c* does not fuse the vesicles while the holoprotein induces fusion at a wide range of pH values[5]. Experiments using a phosphatidylcholine (PC) analogue with a photoreactable hydrophobic label at the head group and another with the label positioned at the end of the acyl chain indicated that the different fusogenic properties of holo- and apoprotein come from the difference in the topology of the membrane penetrating proteins; Apo *c* penetrates deep inside the bilayer while only surface binding occurs for Cyt *c*. However, the experiment with the probes attached to the acyl chains of lipid does not provide an unambiguous result because of the flexible nature of the chains.

Since the topology of the membrane-bound protein may be an important factor for membrane fusion, we have made additional experiments. The two methods used are labeling by phenylisothiocyanate (PITC) in the presence of *p*-sulfophenylisothiocyanate (*p*-sulfo-PITC) and translocation of these proteins across the bilayer of trypsin-entrapped vesicles. PITC is a hydrophobic label which partitions predominantly into the hydrophobic core of the bilayer while *p*-sulfo-PITC is its hydrophilic analogue and thus dissolves in the aqueous phase. The decrease in the labeling by PITC in the presence of *p*-sulfo-PITC is, therefore, a measure of exposure of the protein to the surface. This method was used for the topology studies of erythrocyte band 3 protein and cytochrome *c* oxidase[6,7]. Here we employed the labeling method for comparing the topologies of Cyt *c* and Apo *c* in the bilayer.

Dumont and Richards[8] and Rietveld *et al.*[9] observed that the trypsin entrapped in PC/PS vesicles digests Apo *c* placed outside. They suggested that Apo *c* is hydrolysed inside the vesicles as it is being translocated across the bilayer. Since this is possible only when Apo *c* spans the bilayer and a part of it is exposed to the trypsin inside initially, we repeated the translocation experiments with PS/PE vesicles to compare the topologies.

Experimental

Materials. Phosphatidylserine (PS, from soybean), phosphatidylethanolamine (PE, from bovine brain), Cyt *c* (from horse heart), trypsin (from bovine pancrease), trypsin inhibitor and phenylmethylsulfonylfluoride (PMSF) were purchased from Sigma Chemical Co. Phenyl [^{14}C] isothiocyanate and phenyl-isothiocyanate (PITC) were obtained from Amersham. *p*-Sulfophenylisothiocyanate (*p*-sulfo-PITC) was purchased from Aldrich. All other chemicals were purchased in the highest purity available. Apo *c* was prepared by the silver sulfate method[8]

Vesicle Preparation. The PS/PE (1:1) vesicles were prepared by the reverse phase evaporation (REV) method[10].

Hydrophobic and Hydrophilic Labeling with PITC and *p*-sulfo-PITC. Vesicles (2 mM Pi) were incubated with 5 mg of protein and the binding and reversibility tests were performed as described before[5]. *p*-sulfo-PITC was added to aliquots of the above suspension in differential concentrations. The mixtures were stirred for 1 hour at 37 °C. The modified vesicle-peptide mixtures were then transferred to centrifuge tubes. The mixtures were sedimented for 90 min at 35,000 rpm in a Beckman SW 41 rotor. The supernatants were discarded and the pelleted mixtures were suspended in a buffer. The above washing procedure was repeated twice for the complete removal of unbound *p*-sulfo-PITC. Pellets were resuspended in a buffer and the same concentration of phenyl-[^{14}C]-isothiocyanate was added to each suspension and incubated for 1 hour at 37 °C. The unbound phenyl-[^{14}C]-isothiocyanate was removed by the washing steps described above. The final pellets were solubilized in a buffer containing 1% sodium dodecyl sulfate. Samples were withdrawn from each of these solubilized vesicles for protein determination using the modified Lowry assay[11] at 660 nm and for ^{14}C-counting.

Translocation Assay. Trypsin encapsulated vesicles were prepared by REV method. 1 m*l* of buffer (100 mM NaCl, 10 mM PIPES, pH 7.0) containing 2 mg of trypsin was added to 3 m*l* of diethyl ether containing 3 mg of phospholipid. After 2.5 min of sonication of the dispersion at 4 °C with a probe type sonicator, ether was evaporated by passing N_2 gas at room temperature. Multilamellar vesicles, small unilamellar vesicles and non-encapsulated trypsin were removed by successive centrifugation. To an aliquot (500 μl) of the suspension of trypsin-containing vesicles (corresponding to 2 umole of Pi), 500 μl of trypsin inhibitor (4 $\mu g/\mu l$) was added to inhibit the residual trypsin present outside the vesicles. After 5 min of incubation at 30 °C, the suspension was cooled to 4 °C and divided into several parts. Each portion (volume 54 u*l*, containing 108 nmole of Pi) was incubated with 80 ug of Apo *c* or Cyt *c* at 37 °C in a total volume of 150 u*l*. To determine the extent of protein digestion by trypsin enclosed within the vesicles, each suspension, after different incubation time, was solubilized by mixing with equal volume of a 4% (w/v) sodium dodesyl sulfate solution and immediately heated for 10 min at 100 °C. Urea-SDS-PAGE slab gels were loaded with samples, and electrophoresis was carried out according to the method of Swank and Munkres[12]. The gels were stained with Coomassie Blue R-250 and the intensity of the protein bands was subsequently scanned at 610 nm with a SEBIA FRANCE densitometer. Using the intensity of the trypsin inhibitor band as an internal standard, the amount of protein was estimated from the ratio of the intensities of the protein and trypsin inhibitor bands.

Results and Discussion

The effect of *p*-sulfo-PITC on PITC binding of membrane proteins has two extreme situations. If *p*-sulfo-PITC, at any concentration, does not affect PITC binding, the binding sites are not accessible to the polar *p*-sulfo-PITC. They are therefore most probably located within the hydrophobic interior of the membrane. If *p*-sulfo-PITC pretreatment induces a complete reduction of PITC binding, membrane proteins are located at the surface of the membrane. Fig. 1-a shows that *p*-sulfo-PITC pretreatment of Cyt *c*-vesicle complex induces about 70% reduction of PITC binding to the protein. This suggests that the penetrated fragment of Cyt *c* is located somewhat near the surface. For the case of Apo *c*, however, the reduction of PITC binding induced by pretreatment with *p*-sulfo-PITC brought only about 30% reduction as shown in Figure 1-b. From this result, we may conclude that Apo *c* is located deeper inside.

Figure 2 shows the results of translocation assay. After 3

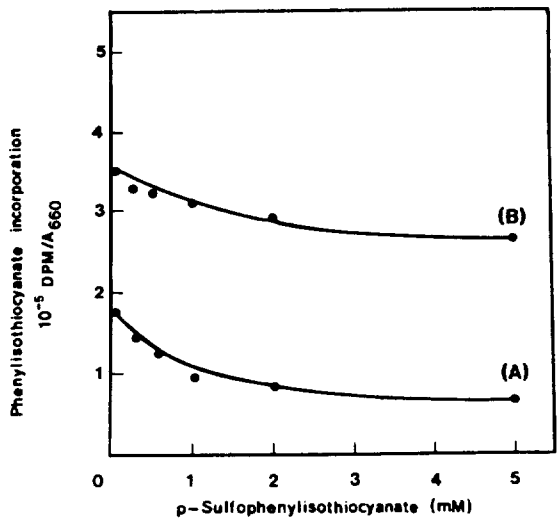

Figure 1. Effect of *p*-sulfo-PITC on the PITC binding to Cyt *c* (A) in the vesicle/Cyt *c* complex, and to Apo *c* (B) in the vesicle/Apo *c* complex. The abscissa represents the total *p*-sulfo-PITC added prior to the addition of PITC.

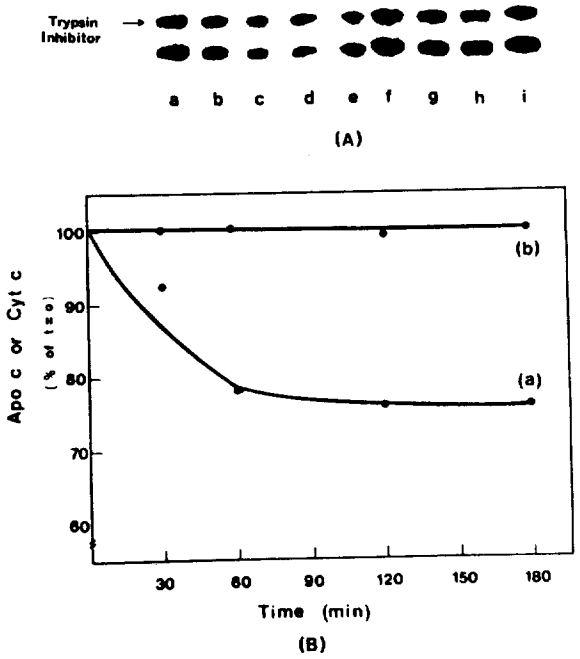

Figure 2. (A) Digestion of Apo *c* and Cyt *c* by trypsin enclosed in PS/PE (1:1) vesicles. To PS/PE (1:1) vesicles with entrapped trypsin, either Apo *c* or Cyt *c* was added and the vesicles were incubated at 37 °C. Sufficient amount of trypsin inhibitor was added to the suspension to prevent digestion of proteins by trypsin attached to the outer surface of vesicles. After 0 min (lanes *a* and *f*), 30 min (*b* and *g*), 60 min (*c* and *h*), 120 min (*d* and *i*) and 180 min (lane *e*), aliquots were drawn and SDS-PAGE was performed. Lower bands shown are Apo *c* (lanes *a-e*) and Cyt *c* (*f-i*). (B) Time courses of Apo *c* (a) and Cyt *c* (b) digestion by trypsin enclosed in PS/PE vesicles.

hours of incubation of Apo *c* with vesicles containing trypsin, about 25% of Apo *c* disappeared. The amount of undigested Apo *c* reached a plateau within 1 hour. This result suggests that some part of the Apo *c* was exposed to the inner space of

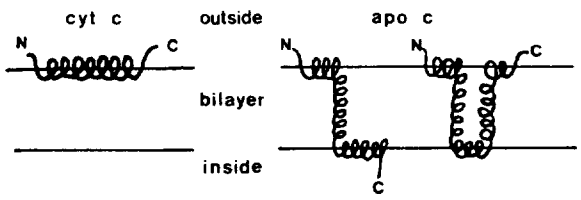

Figure 3. Mode of topologies of Cyt *c* and Apo *c* in the vesicle bilayer.

vesicles initially. For the case of Cyt *c* no translocation occured. This strongly suggests that Cyt *c*, when bound to vesicles, does not traverse the bilayer.

These experiments have shown that the penetrating fragment of Cyt *c* was located mainly on the bilayer surface while that of Apo *c* penetrated deep into the bilayer. From the experimental results so far, we may visualize the possible topologies of penetrated fragments as given Figure 3. It was already demonstrated that a small loop of Cyt *c* is protected from trypsin placed outside of vesicles[5]. Since an α-helix which fully spans the phospholipid bilayer consists of about 25 amino acid residues[13], the loop segment of Cyt *c* goes into the bilayer only a part of way if it forms an α-helix structure. This may mean that the protein loop disturbs only the outer half of a bilayer resulting in the bilayer fusion. Since an α-helical loop penetrating partway into the bilayer is thermodynamically untenable[14], it is likely that the interaction of Cyt *c* with vesicles occurs predominantly on the surface. On the other hand, the protected segment of Apo *c* traverses the lipid bilayer and this is apparently not a favorable topology for inducing fusion. Since the C-terminal region of Apo *c* was not digested either by trypsin or carboxypeptidase Y when Apo *c* is present with vesicles[5], it is not clear whether the C-terminal of Apo *c* is exposed initially to the inner aqueous phase of the vesicles or outside aqueous phase.

The results obtained in the present investigation strengthens the previous conclusion in that Apo *c* penetrates the bilayer much deeper than its holoprotein does and the surface penetration, rather than spanning the bilayer, is crucial to the fusion[5]. The studies on α-lactalbumin-induced fusion[2] and lysozyme-induced fusion[4] generally agree with this notion. This seems also to be true for the case of fusion induced by the BHA protein from the influenza virus envelope, the most studied case of bilogical fusion. It was suggested that the interaction of BHA protein with membrane involves only the external monolayer[15]. How surface penetration of bilayer by a short protein segment, possibly in the α-helical form, can bring about fusion remains to be seen.

Acknowledgement. The financial support of the Korea Science and Engineering Foundation is gratefully appreciated.

References

1. J. Kim and H. Kim, *Biochemistry* **25**, 7867 (1986).
2. J. Kim and H. Kim, *Biochim. Biophys. Acta* **983**, 1 (1989).
3. B. S. Park, J. Kim, U. H. Kim and H. Kim, *Lipids*, **24**, 854 (1989).
4. J. Kim and H. Kim, *Arch. Biochem. Biophys.* **274**, 100

(1989).
5. S. Lee and H. Kim, *Arch. Biochem. Biophys.* **271,** 188 (1989).
6. H. Sigrest, C. Kempf, in A. Azzi, V. Brodbeck, and P. Zahler eds. "Membrane Proteins. A Laboratory Manual", Springer-Verlag, 1981.
7. K. Sigrist-Nelson, H. Sigrest, H. Ariano and A. Azzi, *FEBS Letter* **95,** 140-142 (1978).
8. M. E. Dumont and F. M. Richards, *J. Biol. Chem.* **259,** 4147 (1984).
9. A. Rietveld, W. Jordi, and de B. Kruijff, *J. Biol. Chem.* **261,** 3846 (1986).
10. F. J. Szoka and D. Papahadjopoulos, *Proc. Nat. Acad. Sci. U.S.A.* **75,** 4194 (1978).
11. O. H. Lowry, N. J. Rosebrough, A. L. Farr and R. J. Randall, *J. Biol. Chem.* **193,** 265 (1951).
12. R. T. Swank and K. D. Munkres, *Anal. Bochem.* **39,** 462 (1971).
13. D. M. Engelman and T. A. Steitz, *Cell* **23,** 411 (1981).
14. M. Chabre, *Trends in Biochem. Sci.* **12,** 213 (1987).
15. R. W. Dams and A. Helenius, in S. Ohki *et al.* eds. "Molecular Mechanisms of Membrane Fusion" Plenum, 1988.

Synthesis and Solution Chemistry of Metal Hydrides from Cationic Rhodium(I) Catalyst Precursors $[(L\text{-}L)Rh(NBD)]ClO_4$ (L-L = $Fe(\eta^5\text{-}C_5H_4PBu^t_2)_2$, $Fe(\eta^5\text{-}C_5H_4PPhBu^t)_2$)

Tae-Jeong Kim

Department of Industrial Chemistry, Kyungpook National University, Taegu 702-701. *Received November 10, 1989*

The hydrogenation catalyst precursors $[(L\text{-}L)Rh(NBD)]ClO_4$ (L-L = $Fe(\eta^5\text{-}C_5H_4PBu^t_2)_2$, $Fe(\eta^5\text{-}C_5H_4PPhBu^t)_2$; NBD = norbornadiene) react with H_2(1 atm, 30 °C, MeOH) to yield $[(L\text{-}L)HRh(\mu\text{-}H)_3RhH(L\text{-}L)]ClO_4$. These hydrido species are fluxional, and variable temperature NMR studies show the existence of a number of equilibria involving both fluxional and non-fluxional species. The synthesis, solution structures, and fluxional behaviors of these hydrides are described.

Introduction

One of characteristic features of cationic rhodium(I) hydrogenation catalyst $[(L\text{-}L)Rh(diene)]^+$ (L-L = chelating di(tertiaryphosphine)) is that hydrogenation of this complex results initially in the formation of a disolvate $[(L\text{-}L)Rh(S)_2]^+$ (S = solvent) rather than catalytic hydride(s) commonly found in the case of the monophosphine analogues $[(L)_2Rh(diene)]^+$.[1,2] Brown and coworkers[3], however, have recently shown that hydrogen does add reversibly to $[(dppe)Rh(S)_2]^+$ (dppe = 1,2-bis(diphenylphosphino)ethane), S = MeOH) to give an undetectable concentration of a dihydride $[(dppe)Rh(H)_2(S)_2]^+$. This hydride was formulated as such because Otsuka and coworkers[4] have suggested that this is the composition of the incompletely characterized solids obtained from the reaction of $[(L\text{-}L)Rh(NBD)]ClO_4$ with H_2(L-L = $(C_6H_{11})_2P(CH_2)_4P(C_6H_{11})_2$).

More recently, for the first time, we[5] also reported that metal hydrides are easily obtained from cationic rhodium complexes where L-L is one of a wide range of ferrocenylalkylphosphine $[\eta^5\text{-}C_5H_{5-n}(PR_2)_n]Fe[\eta^5\text{-}C_5H_3(PR_2)C(H)MeNMe_2\text{-}1,2]$ and $Fe(\eta^5\text{-}C_5H_4PR_2)_2$ (R = Bu^t, Pr^i, or Ph:n = 0-2). In two instances hydrides were isolated as stable crystals formulated as $[(L\text{-}L)HRh(\mu\text{-}H)_3RhH(L\text{-}L)]ClO_4$ (**3a**, L-L = $Fe(\eta^5\text{-}C_5H_4PBu^t_2)_2$ (**1a**); **3b**, L-L = $Fe(\eta^5\text{-}C_5H_4PPhBu^t)_2$ (**1b**)). As crystals of **3a** were not good enough to allow the number and disposition of hydrogen atoms to be determined with any certainty, the formulation was based on the charge and the similarity of the overall ligand disposition in the two hydride **3a** and **3b**.

We now provide further evidence for the presence of both terminal and bridging hydrido ligands in **3a** from our NMR studies, along with the description in detail of the synthesis of the two. The NMR spectra of both **3a** and **3b** are complex, and variable temperature studies show the existence of a number of equilibria involving both fluxional and non-fluxional species. These points will also be addressed in this paper.

Experimental

Generals. All manipulations of air-sensitive reagents and products were conducted under an argon atmosphere using a double manifold vacuum system and Schlenk techniques. All commercial reagents were used as received unless otherwise mentioned. Solvents were purified by standard techniques[6], and were freshly distilled prior to use. Hydrogen was passed through a "deoxo" catalytic purifier before use.

Melting points were determined using a Gallenkemp melting point apparatus and are reported without correction. Micro-analyses were performed by Mr. P. Borda of Department of Chemistry, University of British Columbia, Vancouver, Canada. ^1H NMR spectra were recorded on a Bruker WH-400 spectrometer operating at 400 MHz and ^{31}P NMR spectra on Bruker WP-80 or Varian XL-100 spectrometers operating at 32.3 MHz or 40.5 MHz, respectively. All chemical shifts are positive to lower shielding with the following